

1 Comment on “High-Definition Mapping of the Gutenberg–Richter b-Value
2 and Its Relevance: A Case Study in Italy” by M. Taroni, J. Zhuang and W.

3 Marzocchi

4
5 Laura Gulia^{1*}, Paolo Gasperini^{1,2} and Stefan Wiemer³

6
7 ¹ University of Bologna, Department of Physics and Astronomy, Bologna, Italy.

8 ² Istituto Nazionale di Geofisica e Vulcanologia, Bologna, Italy

9 ³ Swiss Seismological Service, ETH Zurich, Switzerland.

10
11
12 L. Gulia: Laura Gulia (laura.gulia@unibo.it)

13 P. Gasperini: Paolo Gasperini (paolo.gasperini@unibo.it)

14 S. Wiemer: Stefan Wiemer (stefan.wiemer@sed.ethz.ch)

15
16 **corresponding author:* Laura Gulia, University of Bologna, Department of Physics and Astronomy,
17 Viale Bertini Pichat, 8 - 40127 Bologna (Italy), laura.gulia@unibo.it

18
19 *The authors acknowledge there are no conflicts of interest recorded*

20
21
22 **Abstract**

23
24 Taroni et al. (2021) published a statistical framework to reliably estimate the b-value and
25 its uncertainties, with the goal being the interpretation in a seismotectonic context and

26 improving earthquake forecasting capabilities. In this comment, we show that the results
27 presented for the Italian region, and the conclusions drawn by the authors, are heavily
28 biased due to quarry blast events in the Italian earthquake catalogue used in the analysis.
29 Without removing this anthropogenic component in the data, a meaningful analysis of
30 the earthquake-size distribution for natural seismicity is, in our opinion, not possible.
31 This comment highlights the need for basic data quality analysis before sophisticated
32 statistical tools are applied to a dataset.

33

34

35

36

37 ***Introduction***

38 Taroni et al. (2021) apply and extend the mapping approach introduced by Tormann et.
39 al. (2014) to analyze the spatial variability of the relative earthquake-size distribution,
40 (the b-value) in Italy. The authors argue that the observed spatial variability has
41 important implications for improving earthquake forecasting capabilities and present
42 also seismotectonic interpretations for the anomalies.

43

44 In our own research of the past 20 years, we likewise have often highlighted the
45 surprising spatial variability of b-values, their link to seismotectonics and stress regimes
46 and their use in earthquake forecasting (e.g., Wiemer and Wyss, 1997; Schorlemmer et
47 al., 2005; Gulia and Wiemer, 2010; Tormann et al., 2015; Petrucelli et al., 2019 a,b; Gulia
48 and Wiemer, 2019). Many other groups have also investigated spatial variations in b-
49 value at all scales (e.g., Enescu and Ito, 2002; Katsumata, 2006; Farrel et al., 2009; Goebel
50 et al., 2013; Schurr et al., 2014; Wu et al., 2018). The analysis presented by Taroni et al.

51 (2021) is in our opinion an important extension of existing mapping techniques;
52 however, we will demonstrate in this comment that sophisticated statistical methods
53 cannot overcome basic limitations and biases posed by the input data. As we show below,
54 the spatial maps of b-values shown in Taroni et al (2021) in their figure 2 do not represent
55 natural earthquakes but map the well-known unusual high b-values of quarry blasts.
56 They hence represent anthropogenic events and cannot be used to infer knowledge on
57 natural seismicity.

58

59

60 ***The influence of quarry blasts on b-values***

61

62 Quarry blasts are in terms of their seismic signals often not easy to distinguish from
63 natural events and increasingly sophisticated processing techniques have been proposed
64 to discriminate them based on waveform analysis (e.g., Allmann et al., 2008; Hammer et
65 al., 2013; Dong et al., 2016; Tan et al., 2020). Quarry blasts also cover a similar magnitude
66 range to micro-earthquakes (Kintner et al., 2021; Gulia, 2010). All seismic networks will
67 strive to identify and flag blast events in their seismicity catalogs, but it is common in all
68 seismic networks that a certain - and sometimes very large fraction - of events is not
69 identified correctly, a fraction that varies by network, with time and with location. It also
70 can happen that the flags are either lost or ignored during catalog analysis steps.

71

72 Wiemer and Baer (2000) introduced a simple statistical test based on the day-to night-
73 time ratio (from now on D/N) to map and potentially remove quarry blast events from
74 earthquake catalogs. For natural earthquakes, the D/N value is typically slightly below 1,
75 due to the lower magnitude detection threshold in night-time that is resulting from the

76 reduced level of anthropic seismic noise (e.g., Hermann et al., 2019). In the presence of
77 anthropogenic events, such as quarry blasts, the D/N ratio increases above 1. In regions
78 of moderate to low natural seismicity, D/N sometimes reaches values >50 (Gulia, 2010),
79 because mine blasts are almost exclusively performed during daytime. A value of 1.5 is
80 already indicative of significant quarry blast contamination (Wiemer and Baer, 2000).
81 Blasts often occur at typical hours in a region, coupled to the work schedule of a quarry,
82 for example 10 am and 4 pm, another characteristic signal for blast contamination. The
83 D/N test has been commonly used in statistical seismology since it was introduced in
84 2000 by Wiemer and Baer (e.g., Godey et al., 2013; Kekovalı and Kalafat, 2014; Gonzales,
85 2017; Giardini et al., 2004; Gulia and Wiemer, 2010; Gulia et al., 2010, 2016, 2018, 2019).
86 Because quarry blasts are not natural earthquakes, they have obviously the potential to
87 bias research on seismicity analysis, such as studies on seismicity rate changes, b-values,
88 fractal dimensions, seismotectonics and earthquake forecasting. Wiemer et al. (2009)
89 pointed out that they also have the potential to impact seismic hazard assessments. Gulia
90 et al. (2012) provided a tutorial on catalog artifacts and quality control as part of the
91 Community Online Resource for Statistical Seismicity Analysis (www.corssa.org),
92 covering quarry explosions a primary example.

93

94 Quarry blasts magnitudes are usually not power law distributed but have similar,
95 'characteristic' sizes, a normal distribution is a better approximation. Consequently,
96 quarry blasts when mixed with a fraction of natural events will exhibit a highly unusual
97 b-value, typically very high ($b > 1.5$), a fact pointed out already by Wiemer and Baer
98 (2000), Wiemer et al. (2009) and Gulia (2010). In a review paper on b-value mapping,
99 Wiemer and Wyss (2000) suggested that contamination by explosion need to be
100 considered and rules out as potential biases.

101

102 The contamination by quarry blasts in the Italian catalogs provided by INGV (as well as
103 other European catalogs) has been investigated by Gulia (2010) and was considered in
104 the CSEP experiment for Italy (Schorlemmer et al, 2010). The maximum magnitude of
105 European quarry blasts is around 2.5 (see Gulia, 2010, and references therein), a value
106 well above the magnitude of completeness adopted by Taroni et al. (2021) for the time
107 interval from 2005 to present (Table 1 in their paper), contamination is thus a possibility
108 to be considered.

109

110

111 ***Quarry blast influence on the Taroni et al. (2021)***

112

113 In their Figure 2, Taroni et al. (2021) show a b-value map for the Italian territory, a second
114 map containing the standard deviation and a third map which combines both b-value and
115 its standard deviation to show only the zones with a b-value significantly different from
116 1.04, the value of the overall catalog. The authors find significantly higher b-values (up to
117 $b = 1.4$) and low standard deviation in three regions: central Apennines, the western part
118 of Tuscany and the northern part of Apulia (yellow areas in their Figure 2c, the map
119 combining b-value with standard deviation) and explain these anomalous high values by
120 referring to the prevalent normal faulting (as suggested by Gulia and Wiemer, 2010) or
121 to the higher heat flux (in particular for Tuscany, Della Vedova et al., 2001).

122

123 To compute these maps, the authors use the H0mogeneous catalog of Italian
124 instRrUmental Seismicity, HORUS (Lolli et al., 2020; available at <https://horus.bo.ingv.it>).
125 It is a composite catalog obtained by merging data from different online resources

126 available for the Italian area; in particular, from 16 April 2005, an automatic procedure
127 periodically downloads the data of the on-line bulletin of the Istituto Nazionale di
128 Geofisica e Vulcanologia (INGV). The events are then automatically homogenized in terms
129 of moment magnitude, while all the other parameters, like location and time, remain
130 unchanged: the potential biases affecting the original data remain in the homogenized
131 catalog.

132

133 We analyzed the effect of blasts on the b-value analysis by Taroni et al. (2021) and show
134 in our Figure 1 the histogram of the daily distribution of events for the highest b-value
135 areas (marked 2, 3, 4). The histograms and the corresponding D/N are computed for
136 circular volumes of 20-km radius (centered in 43.35-13.2, 43.35-13.1 , 40.7-16.7), and
137 shown for two different time periods:

138

- 139 • the entire HORUS catalog (1960-Sept2020) with magnitudes above the value
140 provided in Taroni et al (2021), in order to refer to the same dataset.
- 141 • the time period 16 April 2005 to the end of the catalog, cut at M_c 1.8: this is the
142 part of the catalog with the lowest M_c , thus the more affected by quarry blasts and
143 the richest of small-magnitude events.

144

145 All the three sampled regions exhibit a typical quarry event dominated pattern and a high
146 D/N, ranging from 1.7 to 26, which indicative of very high quarry blast contamination.
147 The dominance of quarry blasts is evident in both periods analyzed. Note that all events
148 used in our analysis and shown in the histograms are above the M_c assumed by Taroni et
149 al. (2021) and thus used in their b-value calculation. Our analysis shown in Figure 1

150 strongly suggests that the observed high b-value anomalies are resulting from
151 anthropogenic events rather than natural earthquakes.

152

153 Taroni et al. (2021) also found high b-values in the western part of Tuscany (labeled 1 in
154 Figure 1). We could not perform a D/N analysis in this volume, because there are actually
155 no events in the catalog here (see Figure 1, inset). We speculate that the analysis by
156 Taroni et al. (2021) samples the fringes of the seismicity in the region. Because small
157 events are often having larger uncertainties in epicenter locations, it is possible that these
158 are scattered beyond the actual extent of the seismicity and fringes will have a size
159 distribution biased towards higher ratios of small earthquakes (Jolly et al., 2007). Such
160 edge-effects are a well-known artifact, the grid sampled thus should be focused closely
161 on active regions (Wiemer and Wyss, 2000), or exclude areas which a large 'gap'. The
162 edge effect is especially clear in the maps shown in the Supplemental Material (Taroni et
163 al., 2021, Figure S1), where a smaller radius (20 km instead of 30) is adopted.

164

165 To further strengthen the argument that the high b-value shown by Taroni et al. (2021)
166 are artifacts, we refer to an independently conducted and recently published study of
167 quarry blast contamination in the Italian earthquake catalog and their impact on b-values
168 by Gulia and Gasperini (2021, in press). Gulia and Gasperini (2021) repeated the same
169 D/N mapping analysis for Italy performed originally by Gulia (2010), showing an overall
170 better performance of quarry-blast discrimination by the Italian network operators.
171 Gulia and Gasperini (2021) then extended the 2010 analysis by also investigating the
172 impact of the quarry blasts, misclassified as natural events, on the b-values in Italy. Areas
173 2, 3, and 4 in our Figure 1 correspond to the areas labeled as F, G and I in Gulia and
174 Gasperini (2021), where the D/N reaches 82 and at the same location very high b-values

175 ($b > 1.5$) are observed. Note that Gulia and Gasperini (2021) performed their analysis on
176 the Italian Seismological Instrumental and Parametric Database, ISIDe (ISIDe Working
177 Group, 2007): it is the source catalog of HORUS for the investigated time interval, so in
178 terms of location, date and time the two datasets are equivalent.

179

180

181 ***Conclusion***

182 Taroni et al. (2021) presented a b-value map for Italy refining the approach by Tormann
183 et al. (2014). However, the application of the methods to map b-values in Italy is in our
184 opinion strongly dominated by quarry blasts and the interpretation presented by the
185 authors that relate high b-values with high heat flux, as well as the implication for the use
186 in earthquake forecasting, are flawed. Quarry blast contamination is a well-known and
187 well-understood phenomenon from more than 20 years (Wiemer and Baer, 2000) that
188 must be considered in all seismicity analyses using events below magnitude 3. Its impact
189 has been documented several times specifically for Italy (Gulia, 2010; Gulia et al., 2012)
190 and it is unfortunate that Taroni et al. (2021) did not consider the available literature or
191 conduct an analysis of the day-to-night-time ratio as a simple quality check. We suspect
192 that other seismicity studies also are biased by quarry explosions, and we welcome
193 efforts by seismic networks to flag these events.

194

195 Because the ability of seismic networks to locate smaller events today is steadily
196 improving, the challenge posed by unrecognized quarry blast contamination may actually
197 increase in some regions. We therefore would like to urge all groups interested in
198 statistical, seismotectonics and seismic hazard related studies to carefully consider
199 anthropogenic events as a potential bias before moving on to ever more sophisticate

200 statistical analysis. We also urge reviewers to request checks of quarry blast
201 contamination for relevant manuscripts. This comment highlights the need for basic data
202 quality analysis before sophisticated statistical tools are applied to a dataset, otherwise
203 the garbage in, garbage out (GIGO) principle applies, meaning that flawed, or nonsense
204 (garbage) input data produces nonsense output.

205

206 ***Response to the reply to our comment:***

207 In their response Taroni et al. compute night-time b-value maps, and we agree that these
208 are a useful additional quality check, in addition to maps of the day to night-time ratio.
209 These maps confirm our assessment that in selected areas, the b-values are
210 overestimated due to quarry blasts.

211

212 In Taroni et al. (2021), the authors perform 3 different maps (Figure 2 a-c in their paper):
213 the b-value map, the standard deviation map and a third map showing only *the b-values*
214 *in the spatial cells in which the b-value computed for the whole catalog falls outside the 95%*
215 *CI of the b-value computed for the spatial cell.* The authors themselves argue that “...*the*
216 *most important one is the third one*”. We would thus have expected in the response to our
217 comment to see the filtered maps, but this was not the case as they only provided (in their
218 Fig. 1) the first kind of maps. As we agree with Taroni et al. (2021) that the most
219 important maps are the filtered ones, we recomputed these maps for the total and night-
220 time catalogs by using the code and data released by the authors with the original paper
221 and provided them here in Figure 2a-f.

222

223 While we agree with Taroni et al. (2021) that in many areas the differences are small,
224 there are in our opinion selected and important places that are very different. In the

225 night-time b-value map with the cells outside the 95% CI (Figure 2f), the quarry blast
226 contaminated area labelled in our comment as 4 disappears entirely and area 3 is
227 substantially reduced, confirming that these high b-value anomalies are pure artifacts.
228 The spatial extent of the area 1 is substantially reduced. Another difference between
229 maps 2c and 2f is the coastal area located just on north of area 1, corresponding in part
230 to the mining district of Apuane, Northern Tuscany: This area disappears in the night-
231 time maps, suggesting that these b-value were computed mainly based on explosion (day-
232 time) events.

233

234 We also note that the maps shown in Figure 2 are computed using large radii (30km) and
235 for long time series (60 years, with decreasing magnitudes of completeness): the effect of
236 blast contamination, often local in space and limited in time, is thus smoothed; for smaller
237 radii (e.g., 20 km, Appendix to Taroni et al, 2021) we would expect to see an even larger
238 difference in b-values between overall and night-time only maps. For area 2 for example,
239 Gulia and Gasperini (2021) show that the b-value changes from 1.4 in the period April
240 2005-April 2012 to 1.2 for the period May 2012-October 2020, due to the better
241 identification of blasts in the last 8 years of the dataset.

242

243 In conclusion, the night-time b-value mapping, especially when focussing on the cells
244 outside the 95% CI, confirms in our opinion that a bias in the analysis by Taroni et al.
245 (2021) was introduced in selected places by quarry blasts. The seismotectonic
246 interpretation and implications for hazard assessment presented in Taroni et al. (2021)
247 must therefore be read with caution for these places.

248

249

250

251 **Declaration of Competing Interests**

252 The authors declare no competing interests

253

254 **Acknowledgments**

255 This study was supported by the Real-time earthquake risk reduction for a resilient
256 Europe (RISE) project, funded by the European Union's Horizon 2020 research and
257 innovation program under Grant Agreement Number 821115 and partially funded by the
258 Pianeta Dinamico-Working Earth INGV-MUR project.

259

260 **Data and Resources**

261 The HOMogeneous catalog of Italian instrumental Seismicity, HORUS (Lolli et al., 2020)
262 is available at <https://horus.bo.ingv.it>.

263

264 **References**

265

266 Allmann B., P. M. Shearer, and E. Hauksson, (2008). Spectral Discrimination between
267 Quarry Blasts and Earthquakes in Southern California, *Bull. Soc. Seim. Am.*, **98**(4),
268 2073-2079.

269

270 Bachmann, C., S. Wiemer, B.P. Goertz-Allmann, and J. Woessner (2012). Influence of pore-
271 pressure on the event-size distribution of induced earthquakes, *Geophys. Res. Lett.*, **39**(9),
272 L09302, doi:10.1029/2012GL051480

273

274 Castello, B., G. Selvaggi, C. Chiarabba, and A. Amato (2006). CSI catalogo della sismicità

275 italiana 1981–2002, versione 1.1, Ist. Naz. di Geofis. E Vulcanol., Rome. (Available at
276 <http://www.ingv.it/CSI/>)
277

278 Della Vedova, B., S. Bellani, G. Pellis, and P. Squarci (2001). Deep temperatures and
279 surface heat flow distribution, in *Anatomy of an Orogen: The Apennines and Adjacent*
280 *Mediterranean basins*, Springer, Dordrecht, The Netherlands, 65–76.
281

282 Dong LJ, J. Wesseloo, Y. Potvin and X.B. Li (2016). Discrimination of mine seismic events
283 and blasts using the Fisher classifier, naive Bayesian classifier and logistic regression,
284 *Rock Mech Rock Eng*, **49**(1), 183–211. <http://dx.doi.org/10.1007/s00603-015-0733-y>
285

286 Enescu, B., Ito, K. (2002). Spatial analysis of the frequency-magnitude distribution and
287 decay rate of aftershock activity of the 2000 Western Tottori earthquake. *Earth Planet Sp*
288 *54*, 847-859, <https://doi.org/10.1186/BF03352077>
289

290 Farrell J., S. Husen, and R.B. Smith, (2009). Earthquake swarm and b-value
291 characterization of the Yellowstone volcano-tectonic system, *J. Volcanol. Geotherm. Res.*,
292 **188**, 260–276
293

294 Giardini D., S. Wiemer, D. Fäh, and D. Deichmann (2004). Seismic hazard assessment of
295 Switzerland, Report, Swiss Seismological Service, ETH Zurich, 88 pp
296

297 Godey, S., R. Bossu, and J. Guilbert (2013). Improving the Mediterranean seismicity
298 picture thanks to international collaborations, *Physics and Chemistry of the Earth, Parts*
299 *A/B/C*, **63**, 3-11, ISSN 1474-7065, <https://doi.org/10.1016/j.pce.2013.04.012>.

300

301 Goebel, T. H. W., D. Schorlemmer, T.W. Becker, G. Dresen and C.G. Sammis (2013).
302 Acoustic emissions document stress changes over many seismic cycles in stick-slip
303 experiments, *Geophys. Res. Lett.*, **40**, 2049–2054. <https://doi.org/10.1002/grl.50507>

304

305 González, Á. (2017). The Spanish National Earthquake Catalogue: Evolution, precision
306 and completeness, *J Seismol.*, **21**, 435–471. [https://doi.org/10.1007/s10950-016-9610-](https://doi.org/10.1007/s10950-016-9610-8)

307 8

308

309 Gulia L. and P. Gasperini, (2021). Contamination of frequency magnitude slope (b-value)
310 by quarry blasts: an example for Italy, *SRL*, in press

311

312 Gulia L. and S. Wiemer (2019). Real-time discrimination of earthquake foreshocks and
313 aftershocks. *Nature*, **574**, 193-199.

314

315 Gulia, L., A.P. Rinaldi, T. Tormann, G. Vannucci, B. Enescu, and S. Wiemer (2018). The effect
316 of a mainshock on the size distribution of the aftershocks, *Geophys Res Lett*, **45**. doi:
317 10.1029/2018GL080619

318

319 Gulia, L., T. Tormann, S. Wiemer, M. Herrmann, and S. Seif (2016). Short-term
320 probabilistic earthquake risk assessment considering time dependent b values, *Geophys.*
321 *Res. Lett.* **43**, 1100–1108, doi: 10.1002/2015GL066686.

322

323 Gulia L., S. Wiemer, and M. Wyss (2012). Catalog artifacts and quality controls,
324 Community Online Resource for Statistical Seismicity Analysis, doi:10.5078/corssa-

325 93722864. Available at <http://www.corssa.org>.

326

327 Gulia, L., S. Wiemer and D. Schorlemmer (2010). Asperity-based earthquake likelihood
328 models for Italy, *Ann. Geophys*, **53**, 3. doi: 10.4401/ag-4843

329

330 Gulia, L., and S. Wiemer (2010). The influence of tectonic regimes on the earthquake size
331 distribution: A case study for Italy, *Geophys Res Lett*, **37**, L10305. doi:
332 10.1029/2010GL043066

333

334 Gulia, L. (2010). Detection of quarry and mine blast contamination in European regional
335 catalogues, *Nat. Hazards*, **53**, 229-249, doi: 10.1007/s11069-009-9426-8.

336

337 Gulia, L., S. Wiemer and D. Schorlemmer (2010). Asperity-based earthquake likelihood
338 models for Italy, *Ann. Geophys*, **53**, no. 3. doi: 10.4401/ag-4843

339

340 Gutenberg, B., and C. F. Richter (1944). Frequency of earthquakes in California, *Bull.*
341 *Seismol. Soc. Am.* **34**, 185–188.

342

343 Hammer, C. M. Ohrnberger, and D. Fäh (2013). Classifying seismic waveforms from
344 scratch: a case study in the alpine environment, *Geophys. J. Int.*, **192**, 425–439.

345

346 Herrmann M., Kraft T., Tormann T., Scarabello L., Wiemer S. (2019). A Consistent High-
347 Resolution Catalog of Induced Seismicity in Basel Based on Matched Filter Detection and
348 Tailored Post-Processing, *J. Geophys. Res.: Solid Earth* **124** (8), 8449-8477.

349

350 Katsumata, K. (2006). Imaging the high *b*-value anomalies within the subducting Pacific
351 plate in the Hokkaido corner. *Earth Planet Sp* **58**, e49–e52,
352 <https://doi.org/10.1186/BF03352640>
353

354 Kekovalı, K., and Kalafat, D. (2014). Detecting of Mining-Quarrying Activities in Turkey
355 Using Satellite Imagery and its Correlation with Daytime to Nighttime Ratio Analysis. *J*
356 *Indian Soc. Remote Sens.*, **42**, 227–232. <https://doi.org/10.1007/s12524-013-0281-4>
357

358 Kintner, J. A. K. M., C.J.A. Cleveland and A. Nyblade (2020). Testing a local-distance Rg/Sg
359 discriminant using observations from the Bighorn region, Wyoming. *Bull. Seismol Soc.*
360 *Am.*, **110**, 727–741
361

362 Jolly, A.D., S.C. Moran, S.R. McNutt and D.B. Stone (2007), Three-dimensional P-wave
363 velocity structure derived from local earthquakes at the Katmai group of volcanoes,
364 Alaska, *J. Volcanol. Geotherm. Res.*, **59** (4), 326-342
365

366 ISIDE Working Group (2007). Italian Seismological Instrumental and Parametric
367 Database (ISIDE), Istituto Nazionale di Geofisica e Vulcanologia (INGV).
368 <https://doi.org/10.13127/ISIDE>
369

370 Petrucci, A., P. Gasperini, T. Tormann, D. Schorlemmer, A. P. Rinaldi, G. Vannucci and S.
371 Wiemer (2019a). Simultaneous dependence of the earthquake-size distribution on
372 faulting style and depth, *Geophys. Res. Lett.* **46**, 20, 11044–11053, doi:
373 10.1029/2019GL083997.
374

375 Petruccioli, A., D. Schorlemmer, T. Tormann, A. P. Rinaldi, S. Wiemer, P. Gasperini and G.
376 Vannucci (2019b). The influence of faulting style on the size-distribution of global
377 earthquakes, *Earth Planet. Sci. Lett.* **527**, doi: 10.1016/j.epsl.2019.115791.

378

379 Petruccioli A., G. Vannucci, B. Lolli and P. Gasperini (2018). *Harmonic fluctuation of the*
380 *slope of the frequency - magnitude distribution (b-value) as a function of the angle of rake,*
381 *Bull. Seismol. Soc. Am.*, **108**, 1864-1876, doi: 10.1785/0120170328.

382

383 Schorlemmer D, A. Christophersen, A. Rovida, F. Mele, M. Stucchi and W. Marzocchi
384 (2010). Setting up an earthquake forecast experiment in Italy, *Ann. Geophys.*, **53** (3):1-9.

385 Available from:

386 <https://www.annalsofgeophysics.eu/index.php/annals/article/view/4844>

387

388 Schorlemmer, D., and S. Wiemer (2005). Microseismicity data forecast rupture area,
389 *Nature*, **434**, 1086, doi:10.1038/4341086a.

390

391 Schurr, B., et al. (2014). Gradual unlocking of plate boundary controlled initiation of the
392 2014 Iquique earthquake, *Nature*, **512**, 299–302, doi:10.1038/nature13681.

393

394 Tan Y. , J. Hu, H. Zhang, Y. Chen, J. Qian, Q. Wang, H. Zha, P. Tang and Z. Nie (2020).
395 Hydraulic fracturing induced seismicity in the Southern Sichuan Basin due to fluid
396 diffusion inferred from seismic and injection data analysis, *Geophys. Res. Lett.* **47**,
397 e2019GL084885.

398

399 Taroni M., J. Zhuang and W. Marzocchi (2021). High-Definition Mapping of the
400 Gutenberg–Richter b-Value and Its Relevance: A Case Study in Italy. *Seismol. Res. Lett.* **XX**,
401 1–7, doi: 10.1785/0220210017.

402

403 Tormann, T., B. Enescu, J. Woessner, and S. Wiemer (2015). Randomness of megathrust
404 earthquakes implied by rapid stress recovery after the Japan earthquake, *Nature Geosci.*
405 **8**, no. 2, 152–158.

406

407 Tormann, T., S. Wiemer, and A. Mignan (2014). Systematic survey of high-resolution b
408 value imaging along Californian faults: Inference on asperities, *J. Geophys. Res.*, **119**, no.
409 3, 2029–2054.

410

411 Wiemer, S., D. Giardini, D. Fäh, N. Deichmann, and S. Sellami (2009). Probabilistic seismic
412 hazard assessment of Switzerland: best estimates and uncertainties, *J. Seismol.*, **13**, 449–
413 478, doi:10.1007/s10950-008- 9138-7.

414

415 Wiemer, S. and M. Baer (2000). Mapping and removing quarry blast events from
416 seismicity catalogs, *Bull. Seism. Soc. Am.* **90**, 2, 525–530

417

418 Wiemer S. and M. Wyss (2000). Minimum magnitude of completeness in earthquake
419 catalogs: Examples from Alaska, the Western United States, and Japan. *Bull. Seism. Soc.*
420 *Am.*, **90**(4), 859–869. <https://doi.org/10.1785/0119990114>

421

422 Wiemer, S. and M. Wyss (1997). Mapping the frequency-magnitude distribution in

423 asperities: An improved technique to calculate recurrence times? *J. Geophys. Research*,
424 102, 15,115–15,128. <https://doi.org/10.1029/97JB00726>

425

426 Wu, Y.-M., S. K. Chen, T. C. Huang, H. H. Huang, W.A. Chao and I. Koulakov (2018).
427 Relationship between earthquake b-values and crustal stresses in a young orogenic belt.
428 *Geophys. Res. Lett.*, **45**, <https://doi.org/10.1002/2017GL076694>

429

430

431 **Authors'adress**

432 Laura Gulia, University of Bologna, Department of Physics and Astronomy, Viale Berti
433 Pichat, 8 - 40127 Bologna (Italy)

434

435 Paolo Gasperini, University of Bologna, Department of Physics and Astronomy, Viale Berti
436 Pichat, 8 - 40127 Bologna (Italy)

437

438 Stefan Wiemer, Swiss Seismological Service, ETH, NO H61, Sonneggstrasse 5, CH-8092
439 Zurich

440

441 **Figure caption**

442

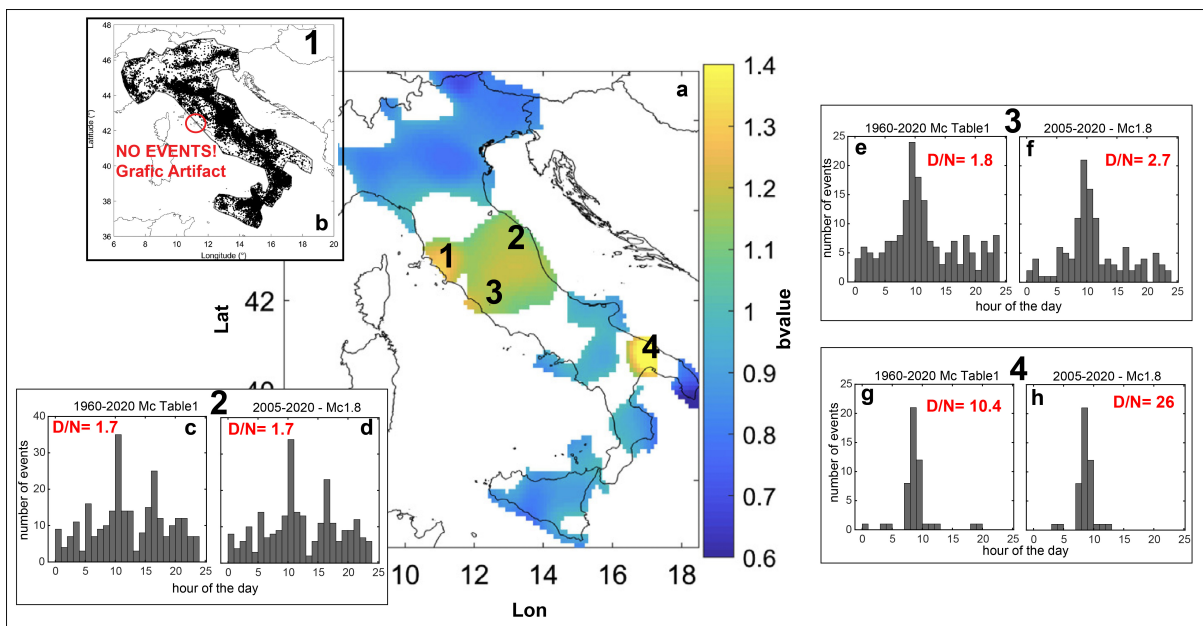
443 **Figure 1** - a) b-value map, modified from Taroni et al. (2021) with, superimposed, the map of the
444 epicenters of events adopted in their paper (b) and, for the sample areas of 20-km radius, in the
445 regions labeled from 2 to 4, the histograms of the hour of events for the whole catalog (c, e and g)
446 and for the time interval 16 April 2005 to the end of the catalog (d, f and h).

447

448 **Figure 2** - a) *b*-Value map for the whole catalog; (b) standard deviation map for the *b*-values in
 449 figure 2a; (c) map for the *b*-values that are significantly different from the one of the whole catalog;
 450 d) *b*-Value map for the night-time events; e) standard deviation map for the *b*-values in figure 2d; f)
 451 map for the night-time *b*-values that are significantly different from the one of the whole catalog.

452
 453

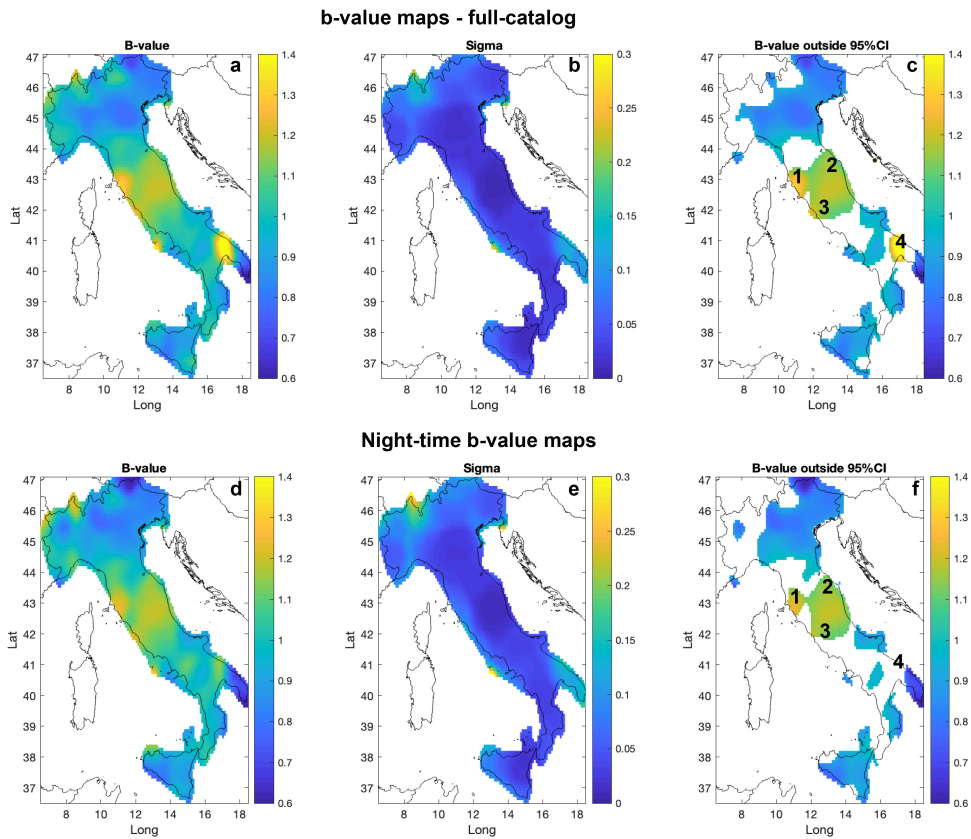
454 **Figure**



455
 456

457 **Figure 1** - a) *b*-value map, modified from Taroni et al. (2021) with, superimposed, the map of the
 458 epicenters of events adopted in their paper (b) and, for the sample areas of 20-km radius, in the
 459 regions labeled from 2 to 4, the histograms of the hour of events for the whole catalog (c, e and g)
 460 and for the time interval 16 April 2005 to the end of the catalog (d, f and h).

461



462

463 **Figure 2** - a) b-Value map for the whole catalog; (b) standard deviation map for the b-values in
 464 figure 2a; (c) map for the b-values that are significantly different from the one of the whole catalog;
 465 d) b-Value map for the night-time events; e) standard deviation map for the b-values in figure 2d; f)
 466 map for the night-time b-values that are significantly different from the one of the whole catalog.

467